BRIEF PAPER *Special Section on Microwave and Millimeter-Wave Technology*

Simple and Tunable MNM by Figure of Eight Resonator and Its Application to Microwave Isolator

Shota KOMATSU[†], ***Student Member and*** **Toshiro KODERA**[†a)], ***Senior Member***

SUMMARY Magnet-less non-reciprocal metamaterial (MNM) synthesise artificial magnetic gyrotropy by metal ring resonator with unilateral component insertion. Clear advantage to natural magnetic material is full integrated circuit ingredient compatibility but still suffers from drawbacks of consumption power in active component and footprint of ring resonator. A new MNM structure by a varactor inserted figure of eight resonator is introduced, which enables reduction of active components by half and even smaller footprint to the original simple ring resonator structure in addition to frequency tunability.

key words: *artificial magnetic gyrotropy, non-reciprocity, magnet-less magnetic metamaterial (MNM), isolator, resonator, traveling-wave*

1. Introduction

Magnet-less Non-reciprocal Metamaterial (MNM) [1]–[3] was presented as an counterpart to biased ferrite [4]. MNM is an artificial electromagnetic metamaterial technology mimicking magnetic gyrotropic properties, and various non-reciprocal microwave devices can be realised in the same manner of conventional microwave ferrite devices [3] without any iron-oxide material but purely consisting of integrated circuit compatible materials. Not only planar component application, MNM also operates *large area* electromagnetic boundary with non-reciprocal polarization shift [1], which is almost unattainable by magnetic material combination. In this paper, improved MNM structure using figure of eight resonator proposed in a single page abstract [5] is developed in order to include detailed principle and design information. The prototype applying the new structure realises higher isolation ratio of more than 20 dB with 2.6 dB insertion loss, those are greatly improved to the original MNM structure [3] of 6 dB isolation with 5 dB insertion loss even with half number of active component and small footprint. In addition, frequency tunability is also realised by varactor diode insertion.

2. Principle of MNM

Figures 1 explain the principle of Magnet-less Non-reciprocal Metamaterial (MNM) [3]. Figure 1(a) shows the unit-cell configuration consisting of uni-directional component inserted metal ring resonator on substrate, where traveling-wave resonance arises under phase matching condition through one-turn propagation. Natural standing wave is reduced by the uni-directional component. The electromagnetic fields in this resonator is excited by the external field through electromagnetic coupling. Figure 1(b) shows the vectorial field explanation of rotating magnetic dipole creation. Electric and magnetic fields of the traveling-wave in the resonator exhibit rotating magnetic field. From macroscopic viewpoint, this internal magnetic field is excited by external electromagnetic field, and they act as magnetisation of this structure. As a result, rotating magnetic dipole moment is excited in this structure, as same as magnetised ferrite.

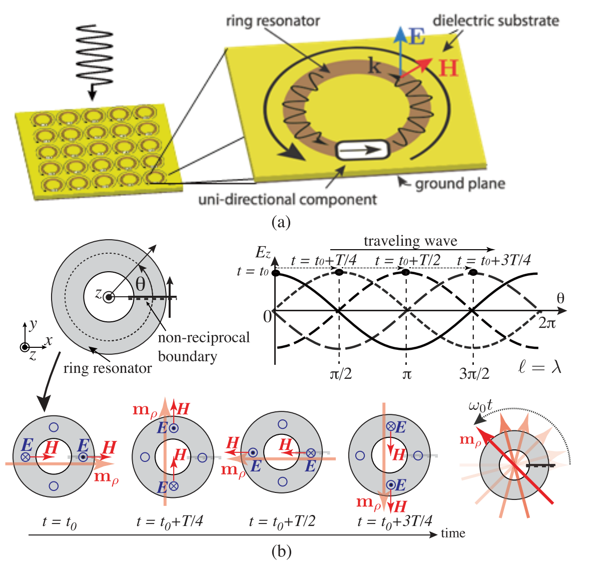

Fig. 1 Principle of Magnet-less Non-reciprocal Metamaterial (MNM). (a) Unit-cell configuration consisting of uni-directional component inserted metal ring resonator on substrate. (b) Vectorial field explanation.

3. Isolator Operation by MNM

By the combination of the artificial magnetic dipole creation and the vector field property of quasi-TEM wave propagation, isolator operation is realised. Figure 2 shows general quasi-TEM wave propagation in microstrip line. Propagating wave accompanies electric fields normal to substrate and magnetic field has a in-plane closed loop. Following magnetic field at fixed position, we can see counter clockwise (CCW) rotating magnetic field excitation on the

Manuscript received February 5, 2016.
Manuscript revised May 13, 2016.
[†]The authors are with the Department of Interdisciplinary Science and Engineering, Meisei University, Hino-shi, 191–8506 Japan.
a) E-mail: toshiro.kodera@meisei-u.ac.jp
DOI: 10.1587/transele.E99.C.1215

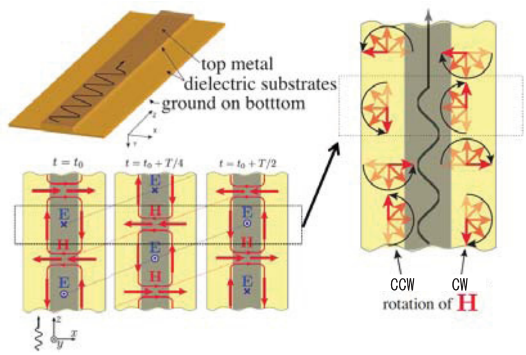

Fig. 2 General quasi-TEM wave propagation in microstrip line.

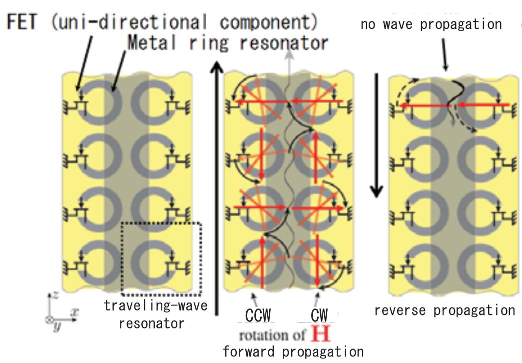

Fig. 3 Principle of isolator operation using MNM.

left side toward propagation, and clockwise (CW) rotating field on right side [6]. Considering the vectorial field in Fig. 2, let us see the case with MNM. Figure 3 explains the principle of isolator operation using MNM. Traveling-wave resonators are arranged on left and right-hand sides below wide microstrip line (MSL) acrossing vertically. This main MSL is connected device ports, and RF power are excited from them. In the case of upward excitation, rotating magnetic field generated along wave propagation, as described in Fig. 2, is co-directional that in traveling-wave resonator, leads to passing operation. In the case of downward excitation, rotating field through propagation is counter-directional to that in traveling-wave. In this case, all of traveling-wave does not support wave propagation, rather resists it, leads to rejection operation for reverse propagation. By these vectorial effect, isolator property is obtained. Figure 4 shows the isolator configuration based on the principle in Fig. 3. Right figure shows total device appearance and left one shows the structure below main MSL connecting port #1 and 2. Each of FET have two ohmic resisters (68Ω and 100Ω) for impedance matching to ring resonator, and bias line consisting of lumped element choke coil, meander line, and by-pass capacitor for stability. The dielectric constant of the substrate ε_r is 2.6 with 0.8 mm thick. Figure 5 shows the prototype device of Fig. 4, and transmission characteristics are shown in Fig. 6. Figure 6(a) plots the simulated value between ports, where isolation ratio ($|S_{21}|-|S_{12}|$) has a poor value less than 10 dB. This value can

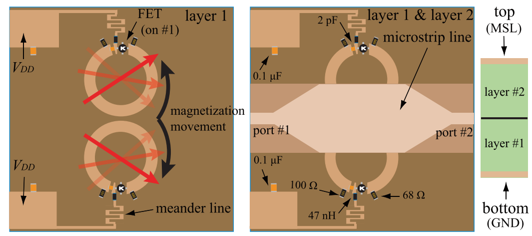

Fig. 4 Isolator configuration based on the principle in Fig. 3.

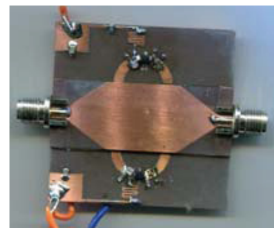

Fig. 5 Picture of prototype isolator corresponds to Fig. 4.

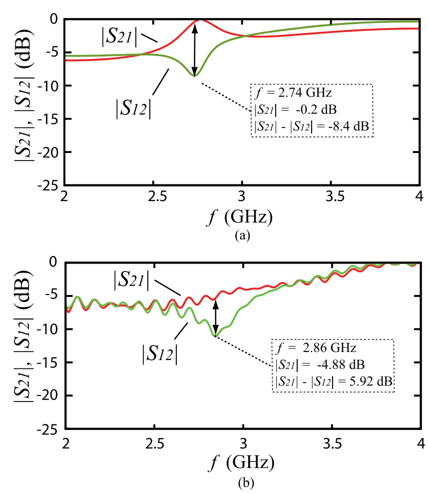

Fig. 6 Transmission characteristics of the isolator in Fig. 4. (a) Simulation results. (b)Measured value.

be improved by adding rows of ring resonators [3], but the corresponding measured value in Fig. 6(b) also shows just 6 dB isolation. This fact, two active component consumption with 6 dB isolation is never acceptable for practical application. As a solution to this poor performance, "figure of eight" MNM is considered.

4. Isolator Based on Figure of Eight Resonator

The proposed structure is shown in Fig. 7, where right figure shows total device appearance and left one shows the structure below main MSL connecting port #1 and 2. It consists of varactor inserted figure of eight resonator, where two rings are connected with two level crossing and sharing one unilateral component. FET and varactor diode are biased through meander and RF choke. Port #1 and #2 are connected by tapered microstrip line over the resonator sepa-

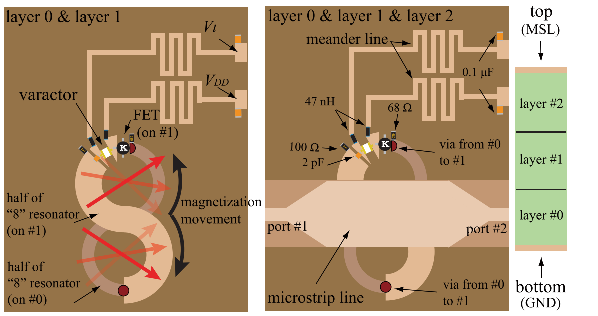

Fig. 7 Tunable microwave isolator using figure of eight resonator, consisting of varactor inserted figure of eight resonator over two layers. The ring is organised in two layers, and as a consequence one layer is added to Fig. 4.

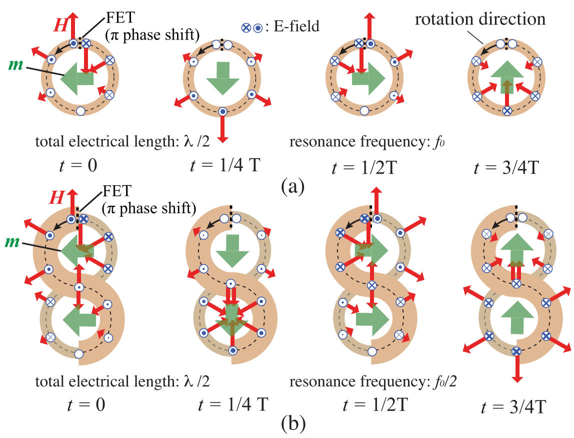

Fig. 8 Vectorial fields comparison of magnetic field in FET inserted (a) simple ring resonator and (b) figure of eight ring resonator for one harmonic period, assuming 180° phase shift FET is inserted on the top of figures.

rated by dielectric substrate. The dielectric constant of the substrate ε_r is 2.6 with 0.8 mm thick. In order to see its operation, vectorial fields comparison of magnetic field in FET inserted (a) simple ring resonator and (b) figure of eight ring resonator for one harmonic period in the case of fundamental (1st) resonance are illustrated in Figs. 8. The small arrows on the ring corresponds to magnetic field and their length and direction correspond to linear amplitude and sign in each position. The large thick arrow inside ring particle corresponds to vectorial summation *direction* of each part. It should be noted that, the total electrical length of (a) and (b) are the same but physical length of (b) is twice as (a), leading *half resonance frequency for a fixed footprint*. As is shown in Fig. 2, each rings across main MSL should have out-of-phase and the structure (b) enforces the situation by its structure. This configuration gives more ideal vectorial fields for isolator realisation, leading higher rejection ratio than the structure (a).

Figure 9 shows the division of figure of eight resonator for operation frequency design. The figure of eight ring structure extends four parts including (1) MSL on dielectric substrate having $2t$ thickness, (2) strip line inside dielectric, aparted from ground by t, (3) strip line aparted from ground

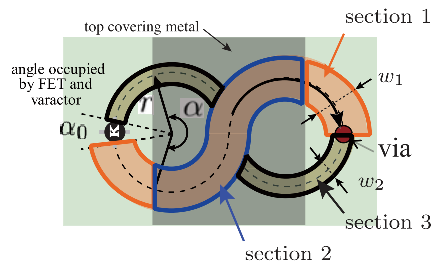

Fig. 9 Division of figure of eight resonator for design.

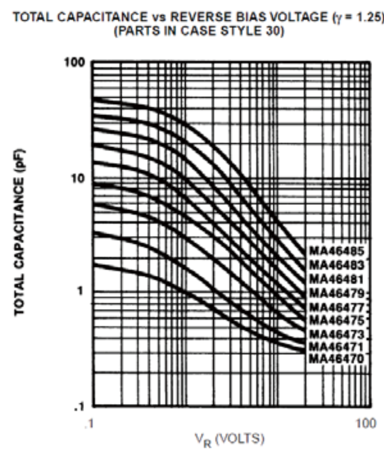

Fig. 10 Varactor diode (MA46470) response for reverse voltage in [7].

by $2t$. To be exact, region (3) includes additional two parts and region (2) includes one additional part but these regions are assumed to be single section for design simplicity. w_1 and w_2 are determined for 50Ω line impedance. Considering phase constant of each sections, the resonance frequency of the ring ω, i. e. operation frequency of MNM is estimated by the following equation,

$$\omega = \frac{c(2\pi - \phi_0 + \phi_{\mathrm{varactor}})}{r[\sqrt{\varepsilon_r}(2\pi + \alpha - \alpha_0/2) + \sqrt{\varepsilon_e}(2\pi - \alpha - \alpha_0/2)]} \quad (1)$$

, where c is speed of right, r is center radius of ring particle, ε_r is the relative permittivity of substrate, ε_e is the effective permittivity of MSL, α defines the overlapped region in Fig. 7, and α_0 is the angle occupied by FET and varactor as in Fig. 7. ϕ_{varactor} is a phase shift in varactor, which can be estimated by $\phi_{\mathrm{varactor}} = -\arctan(1/(2\omega CR))$, where C is the varactor capacitance and R is the loaded impedance, 50Ω. Considering feasible capacitance variation from 0.3 to 2pF, frequency tunable range is designed from 4.2 to 4.6 GHz. The whole structure of Fig. 7 is prepared in simulation model by the commercial simulator (*CST Microwave Studio*). The varactor part is simply modeled by variable capacitance from 0.3 pF to 2.0 pF, which corresponds to reverse voltage variation from 0.1 to 18 V, which can be read in actual device (MA46470) datasheet in Fig. 10. Figure 11 shows the prototype picture corresponds to Fig. 7. Measured and simulation values are compared in Fig. 12 for

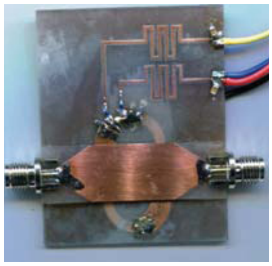

Fig. 11 Picture of prototype isolator corresponds to Fig. 7.

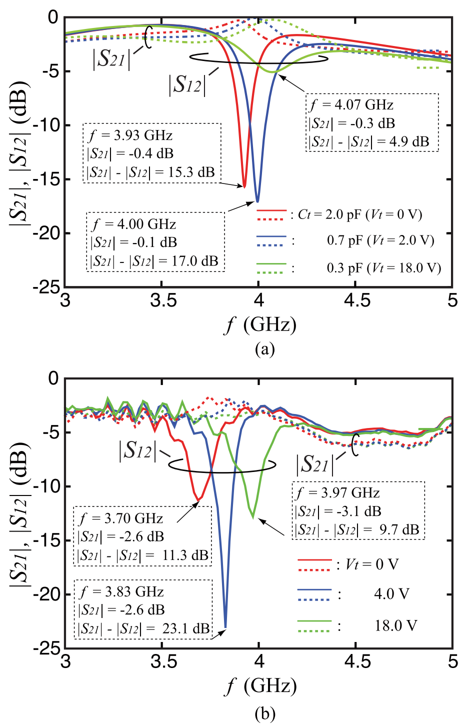

Fig. 12 Transmission characteristics of the prototype isolator in Fig. 7. (a) Simulation results. (b) Measured value obtained by the device in Fig. 11.

various varactor bias voltage. Figure 12(a) shows the simulated transmission characteristics for C_t variation from 2.0 to 0.3 pF. As it can be clearly seen that, the isolation ratio is greatly improved compared to the case in Fig. 6(a). Figure 12(b) shows the measured frequency response of the prototype in Fig. 11. The tuning range of 200 MHz by 18 V tuning voltage variation is realised with clear non-reciprocity. It should be noted that, the realised isolation (23.1 dB) is far better than the two ring original MNM isolator (5.9 dB) in Fig. 6(b), which is due to the fact that half of 8-resonator are *always* out-of-phase for $\lambda/2$ resonance. This phase relation provides more complete closed magnetic field line below main microstrip structure, those are fundamental requirement to obtain isolator operation [3].

5. Conclusion

A new MNM structure by a varactor inserted figure of eight resonator is introduced, which enables reduction of active components by half and even smaller footprint to the original simple ring resonator structure in addition to frequency tunability keeping better frequency response to the original.

Acknowledgements

This work has been carried out under the sponsorship of KAKENHI # 26289106.

References

[1] T. Kodera, D.L. Sounas, and C. Caloz, "Artificial Faraday rotation using a ring metamaterial structure without static magnetic field," Appl. Phys. Lett., vol.99, pp.031114:1-3, July 2011.

[2] D.L. Sounas, T. Kodera, and C. Caloz, "Electromagnetic Modeling of a Magnetless Nonreciprocal Gyrotropic Metasurface," IEEE Trans. AP, vol.61, no.1, pp.221–231, Jan. 2013.

[3] T. Kodera, D.L. Sounas, and C. Caloz, "Magnetless Nonreciprocal Metamaterial (MNM) Technology: Application to Microwave Components," IEEE Trans. MTT, vol.61, no.3, pp.1030–1042, March 2013.

[4] B. Lax and K.J. Button, Microwave Ferrites and Ferrimagnetics, McGraw-Hill, 1962.

[5] S. Komatsu and T. Kodera, "Compact and tunable MNM by figure of eight resonator and its application to microwave isolator," Proc. Int. Conf. of Metamaterials, Photonic Crystals and Plasmonics (META '15), one-page, Aug. 2015.

[6] J. Adam, L. Davis, G. Dionne, E. Schloemann, and S. Stizer, "Ferrite devices and materials," IEEE Trans. Microwave Theory Tech., vol.50, no.3, pp.721–737, March 2002.

[7] M/A COM. inc. MA46410 data sheet. http://www.rf-microwave.com/datasheets/4822_MA-COM_MA46470-276_01.pdf. (accessed 2016-02-5)